Science Advances
AAAS

Supplementary Materials for

A large-scale transcontinental river system crossed West Antarctica during the Eocene

Maximilan Zundel *et al.*

*Corresponding author Cornelia Spiegel. Email: cornelia.spiegel@uni-bremen.de

This PDF file includes:

Supplementary Figs. S1 to S9

Other Supplementary Materials for this manuscript include the following:

A spreadsheet with the supplementary tables

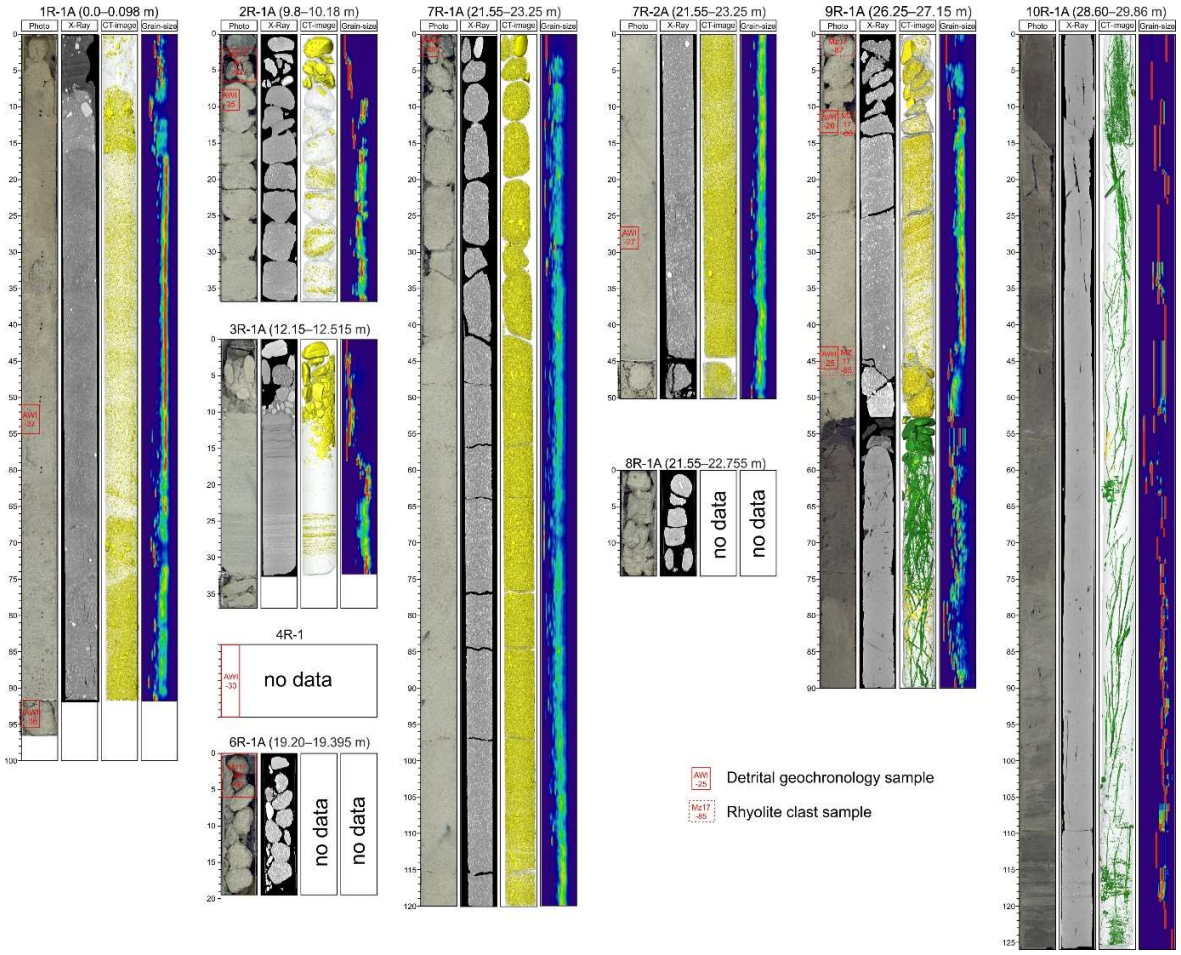

Fig. S1.

Scans and grain-sized distribution from recovered core sections of site PS104_20-2. CT-images show particles >1 mm in yellow while lignite fragments and roots are displayed in green. Grain-size distributions are scaled in phi values from -7 (left) to -1 (right), but need to be treated with care. Note that the number of clasts >1 mm below the hiatus (contained in segment 9R-1A) is very low.

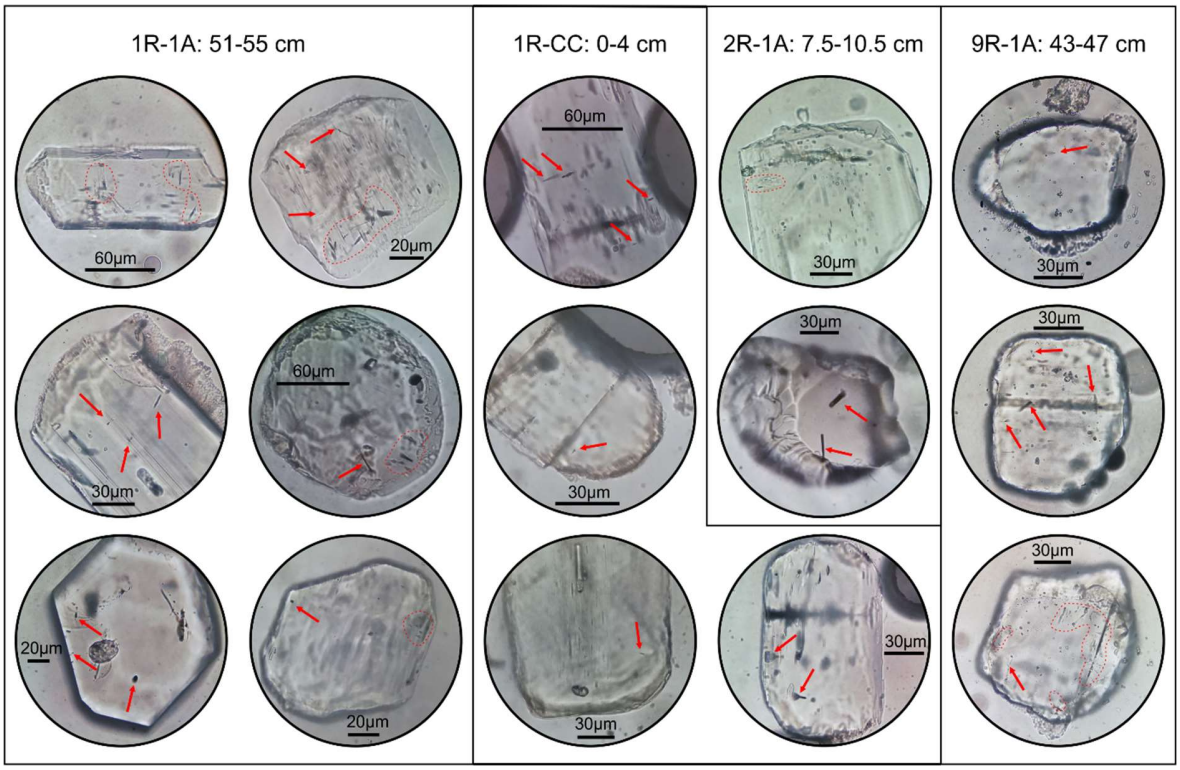

Fig. S2.

Figure shows individual apatite crystals which reveal naturally etched fission tracks and other crystal defects. Locations of these features are highlighted by red arrows and red dashed lines, respectively. Photomicrographs were taken of internal surfaces of apatite mounted in epoxy through an optical microscope at 1000x magnification with transmitted light.

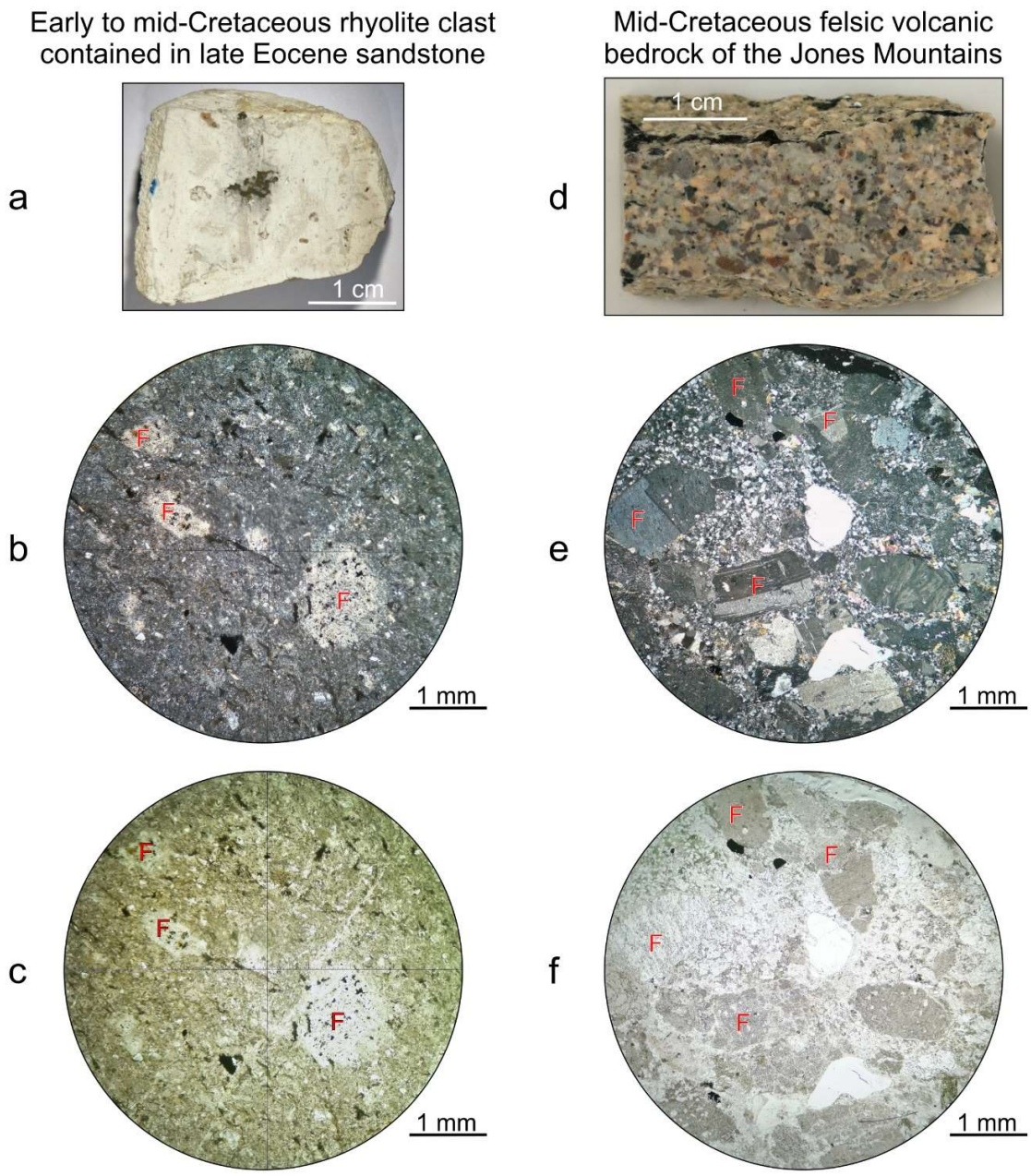

Fig. S3.

Petrographic comparison of rhyolite clasts from the Polarstern Sandstone (a–c) and from bedrock of the Jones Mountains (d–f). Hand specimens are shown in a) and d). The photomicrographs show the alteration state of feldspars (F) in cross-polarized light (b, e) and in plane-polarized light (c, f)

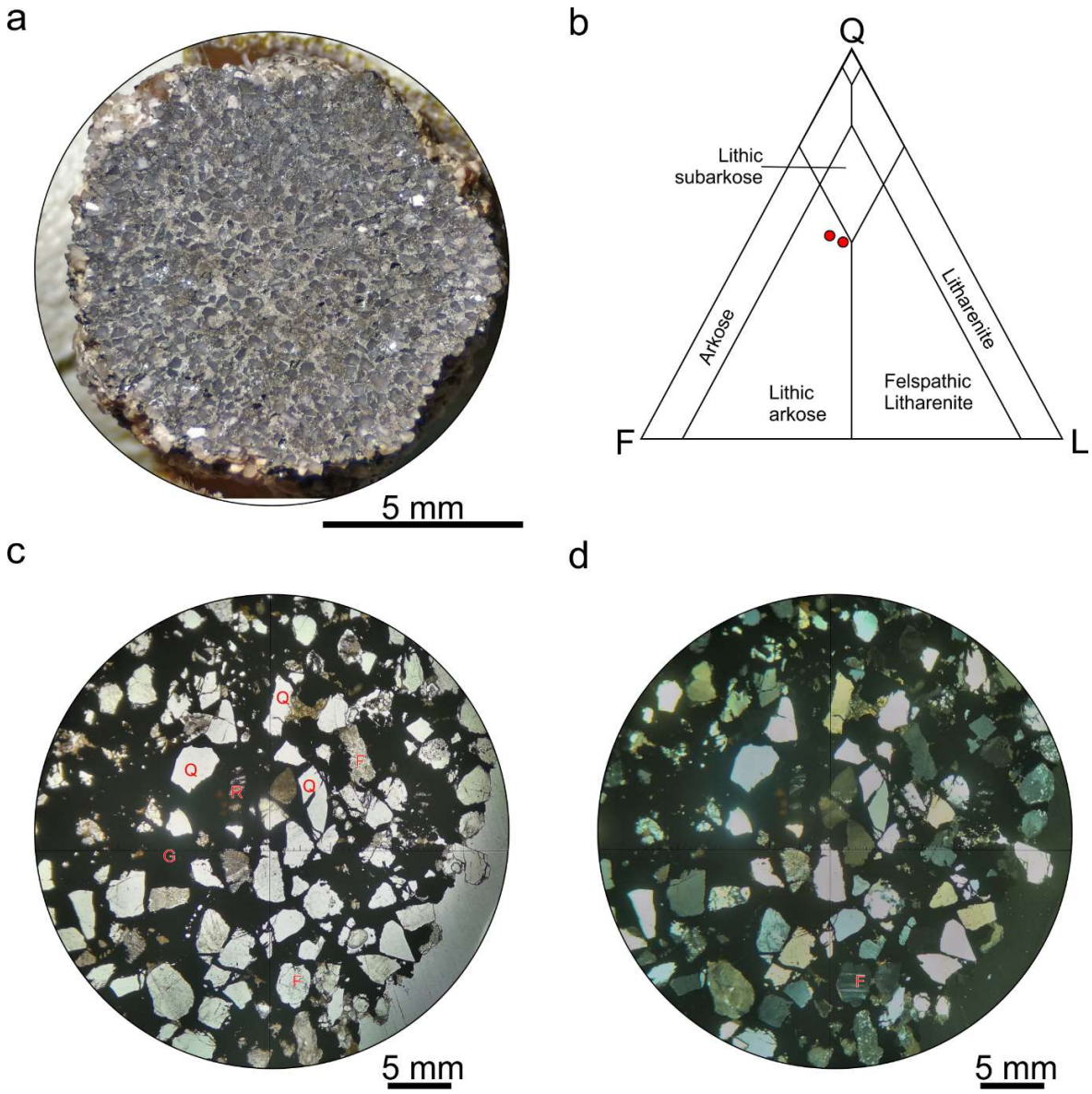

Fig. S4.

Characterization of lithic arkose pebbles contained in the Polarstern Sandstone (at 26.37 and 23.04 mbsf). a) Pebble with angular grains embedded in fine-grained Fe-rich groundmass. b) Quartz-Feldspar-Lithic fragment (QFL)-diagram in which the sandstone pebbles (red dots) are classified as lithic arkoses based on data obtained by point-counting (see Material and Methods). c) Plane-polarised photomicrograph showing individual components of the lithic arkose pebble. Q=quartz; F=feldspar; L=lithic clasts; G=groundmass. d) Corresponding cross-polarised micrograph of c).

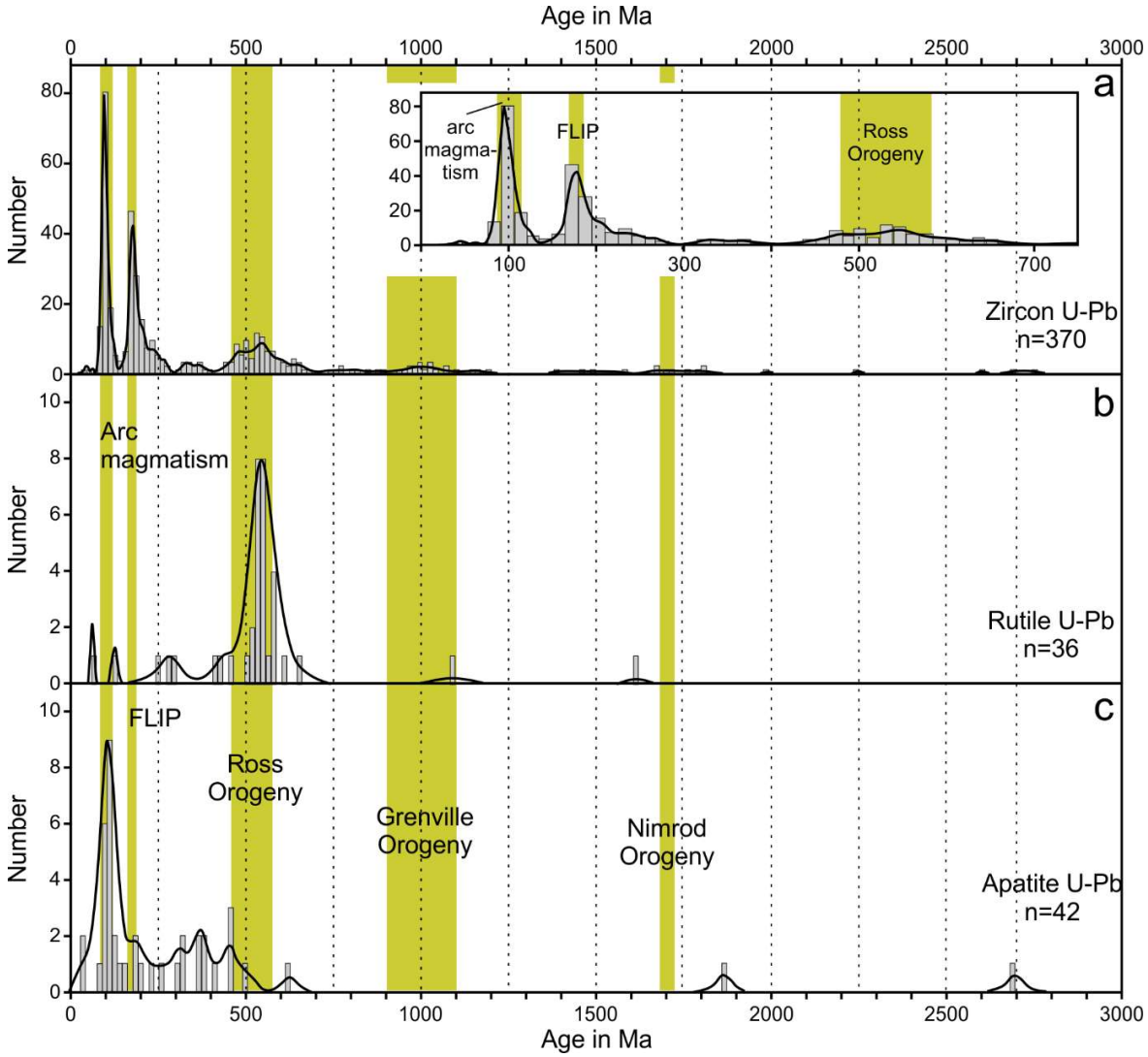

Fig. S5.

Histogram and probability distribution curves of U-Pb ages retrieved from detrital zircon (a), rutile (b), and apatite (c). Major magmatic events and orogenies are also indicated. FLIP = Ferrar Large Igneous Province.

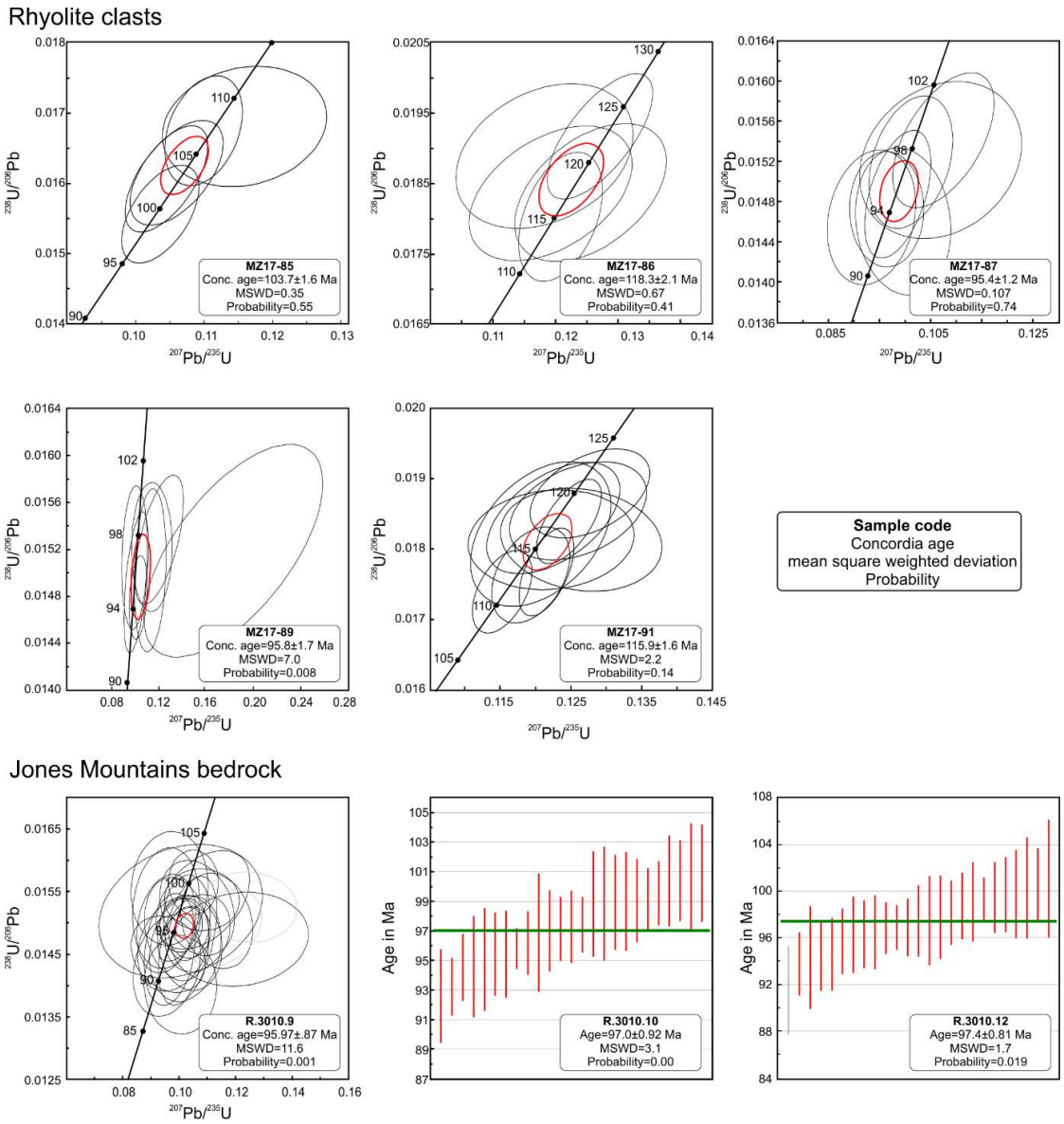

Fig. S6

Concordia plots of zircon U-Pb data for rhyolite pebbles contained in the middle to late Eocene Polarstern Sandstone (upper panels) and for bedrock volcanic and volcaniclastic rocks from the Jones Mountains (lower panels). The red ellipse represents the concordia age. Note that ages displayed for samples R.3010.10 and R.3010.12 are weighted mean single-grain concordia ages.

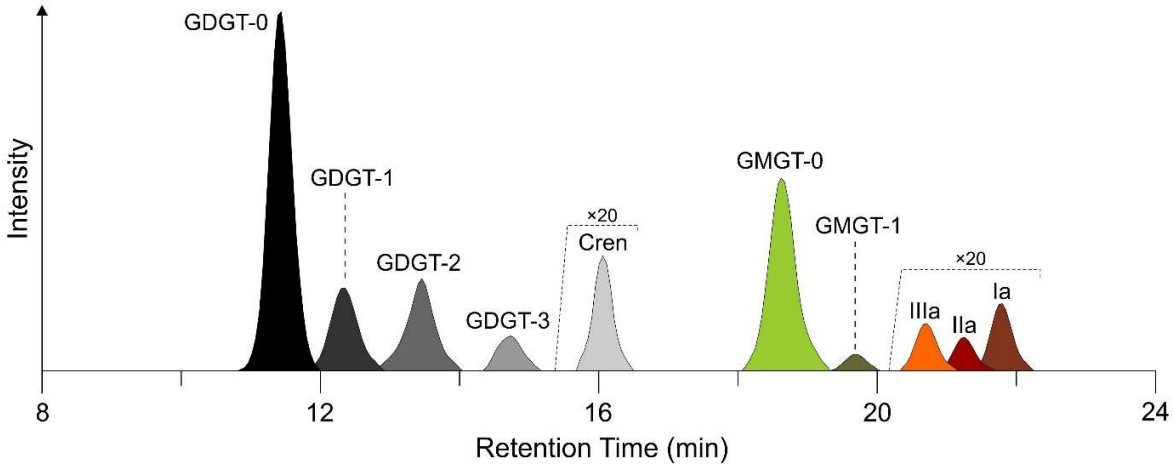

Fig. S7.

Composite mass chromatogram showing the distribution of archaeal and bacterial tetraethers in the Polarstern Sandstone. Cren = crenarchaeol; GDGT= glycerol dialkyl glycerol tetraether; GMGT = glycerol monoalkyl glycerol tetraether. Numbers indicate the amount of cyclopentane rings in the molecule structure. Roman numerals refer to the different bacterial-derived GDGTs (Ia, IIa, IIIa) detected in the sandstone.

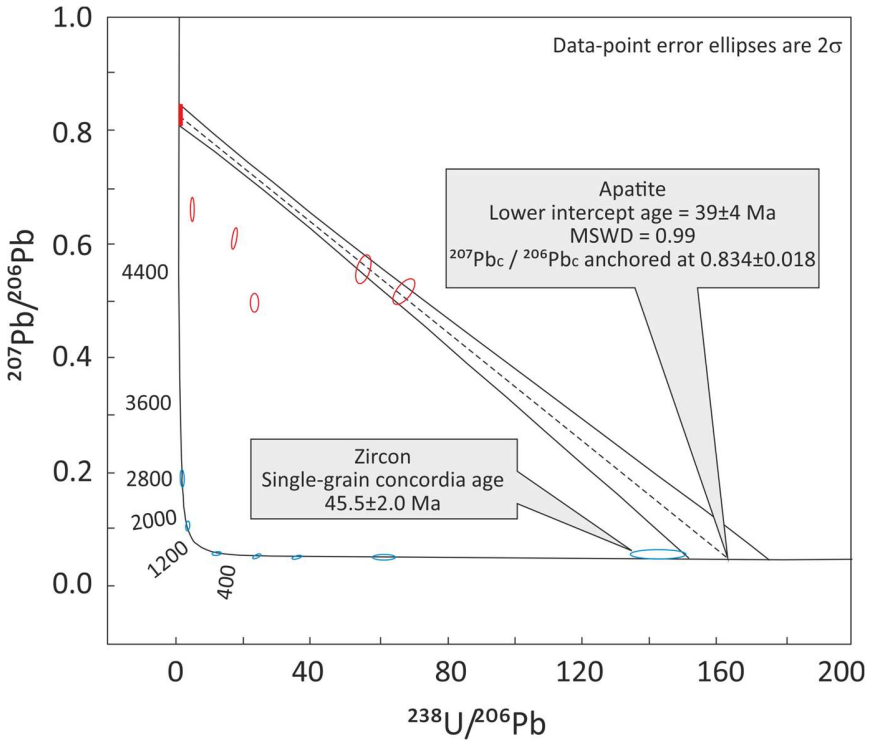

Fig. S8.

Tera-Wasserburg diagram showing apatite (red; 9.9 mbsf) and zircon (blue; 26.7 mbsf) U-Pb data. Red bar at upper array intercept for Eocene apatite is the range of crystalline basement $^{207}Pb_c/^{206}Pb_c$ values for West Antarctica (61), which anchor the apatite age calculation.

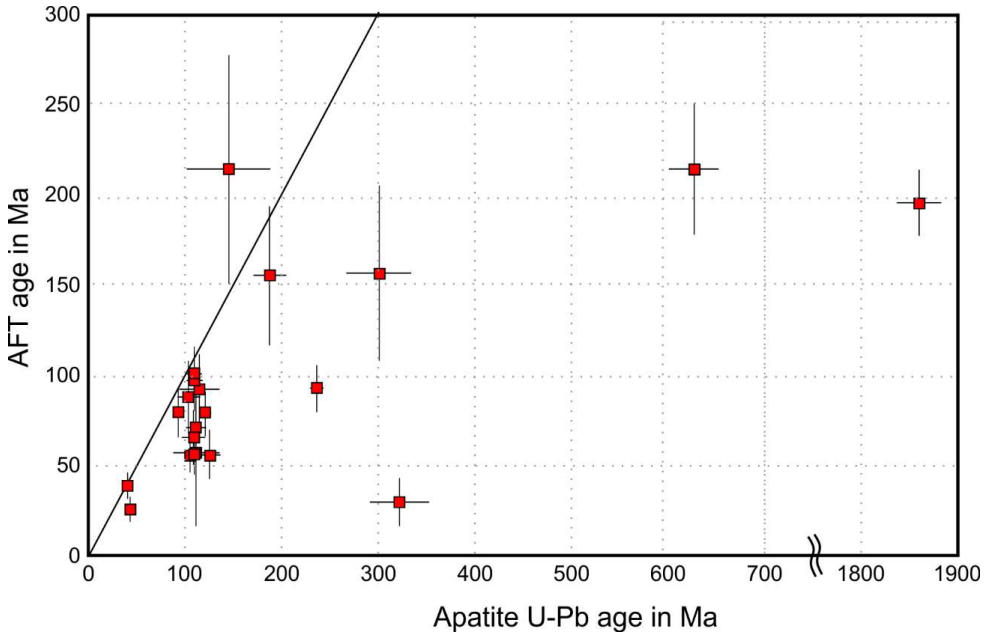

Fig. S9.

Plot showing U-Pb age vs AFT age for all double-dated detrital apatite grains. Black line connects points of equal U-Pb and AFT age. U-Pb and AFT error bars are 2σ and 1σ, respectively.